Organic Electronics 42 (2017) 34–41

Contents lists available at ScienceDirect

Organic Electronics

journal homepage: www.elsevier.com/locate/orgel

Enhanced photovoltaic performances of bis(pyrrolo[3,4-c]pyrrole-1,3-dione)-based wide band gap polymer via the incorporation of an appropriate spacer unit between pyrrolo[3,4-c]pyrrole-1,3-dione units

Vellaiappillai Tamilavan [a, b], Seungmin Kim [b], Jiyeong Sung [a], Dal Yong Lee [b], Shinuk Cho [c], Youngeup Jin [d], Junghyun Jeong [b], Sung Heum Park [b, **], Myung Ho Hyun [a, *]

[a] Department of Chemistry, Chemistry Institute for Functional Materials, Pusan National University, Busan 690-735, Republic of Korea
[b] Department of Physics, Pukyong National University, Busan 608-737, Republic of Korea
[c] Department of Physics, Ulsan University, Ulsan 680-749, Republic of Korea
[d] Department of Industrial Chemistry, Pukyong National University, Busan 608-739, Republic of Korea

ARTICLE INFO

Article history:
Received 4 October 2016
Received in revised form
29 November 2016
Accepted 4 December 2016
Available online 8 December 2016

Keywords:
Polymer solar cells
Spacer unit effects
Benzodithiophene-based polymers
Pyrrolo[3,4-c]pyrrole-1,3-dione-based polymers
Imide functionalized polymer

ABSTRACT

Bis(pyrrolo[3,4-c]pyrrole-1,3(2H,5H)-dione) (BDPPD)-based new electron deficient monomer unit (TTBDPPD) incorporating thieno[3,2-b]thiophene as a connecting spacer unit in between pyrrolo[3,4-c]pyrrole-1,3(2H,5H)-dione units was prepared. The copolymerization of 2D-conjugated benzodithiophene (BDTT) and TTBDPPD derivatives afforded new alternating copolymer P(BDTT-TTBDPPD). The estimated optical band gap and highest occupied molecular orbital (HOMO)/lowest unoccupied molecular orbital (LUMO) energy levels of P(BDTT-TTBDPPD) were 2.06 eV and −5.42 eV/−3.36 eV, respectively. The organic field effect transistor made form P(BDTT-TTBDPPD) exhibited a hole mobility of 6.21×10^{-4} $cm^2V^{-1}s^{-1}$. The polymer solar cells (PSCs) prepared using P(BDTT-TTBDPPD):$PC_{70}BM$ (1:2 wt %)+3 vol% DIO blend offered a maximum power conversion efficiency (*PCE*) of 5.37% with an open-circuit voltage (V_{oc}) of 0.90 V, a short-circuit current (J_{sc}) of 8.94 mA/cm^2 and a fill factor (*FF*) of 67%. This study reveals that the photovoltaic performance of BDPPD-based reported polymer, P(BDTT-TBDPPD), incorporating thiophene spacer unit in between pyrrolo[3,4-c]pyrrole-1,3(2H,5H)-dione units has been greatly improved (over 2%) when thiophene replaced with thieno[3,2-b]thiophene.

1. Introduction

Developing efficient semiconducting polymers [1–6] has been shown great attention for polymer solar cells (PSCs) application because of the world energy needs. The easy device fabrications of PSCs via the solution processability, light weight and low cost to large area device preparation make it a highly efficient solar to electrical energy conversion technique [1–6]. The photoactive layers of PSCs, which are used for light harvesting and charge separation, have been usually made from the blends of electron donating polymer and electron accepting fullerene derivative [1–6]. It is well documented that the properties such as absorption, energy levels, carrier mobility, orientation, molecular weights and crystallinity of electron donating polymer, and the nano scale interpenetrating network between polymer and fullerene derivative play a vital role on the photovoltaic performance of PSCs [1–6]. The electron deficient [6,6]-phenyl-C71-butyric acid methyl ester (PC70BM) is set to be a most promising acceptor and the conventional PSCs made using polymer and PC70BM offered a PCE over 10% [7–18]. Therefore, researchers focused on the preparation of structurally new efficient donor polymers to improve further the device performances of PSCs. Recently physicist introduced tandem and ternary PSCs which are made from two different polymers possess dissimilar absorption and energy levels with the aim of improving the PCE of conventional PSCs [19–30]. The tandem [19–24] and ternary [25–30] PSCs also exhibited a maximum PCE over 10%. The careful literature search indicates that there are numerous efficient low (E_g ~ 1.3–1.6 eV) [1–12] and medium (E_g ~ 1.6–1.9 eV) [1–6,13–18] band gap polymers reported for PSCs but efficient wide band gap polymers (E_g > 1.9 eV) [31–35] are

* Corresponding author.
** Corresponding author.
E-mail addresses: spark@pknu.ac.kr (S.H. Park), mhhyun@pusan.ac.kr (M.H. Hyun).

http://dx.doi.org/10.1016/j.orgel.2016.12.012
1566-1199/

limited. It is necessary to develop structurally new high energy converting wide band gap polymers to explore more on tandem and ternary PSCs.

In this instance, recently we reported imide functionalized bis(pyrrolo[3,4-c]pyrrole-1,3(2H,5H)-dione) (BDPPD)-based wide band gap polymers for PSCs [36]. Actually, thiophene incorporated BDPPD (TBDPPD) unit was prepared and copolymerized with benzodithiophene (BDT and BDTT) derivatives to afford polymers P(BDT-TBDPPD) and P(BDTT-TBDPPD). The absorption band of P(BDT-TBDPPD) and P(BDTT-TBDPPD) was found to cover the region from 300 nm to 600 nm, and the maximum PCE was 2.74% and 3.63%, respectively [36]. Usually, imide functionalized polymers [2,34,35,37–40] were found to exhibit high photovoltaic performances mainly because of the enhanced planarity through the conformational locking due to the S–O interactions between the thienyl sulfur (S) on adjacent electron rich units and the carbonyl oxygen (O) on the imide groups [2,37]. However, imide functionalized polymers P(BDT-TBDPPD) and P(BDTT-TBDPPD) showed relatively poor photovoltaic performances. The lack of the S–O interactions between the thienyl sulfur (S) and the carbonyl oxygen (O) on TBDPPD unit could be a reason for the decreased PCE for P(BDT-TBDPPD) and P(BDTT-TBDPPD). The chemical structure of P(BDTT-TBDPPD) along with the possible S–O interactions on its backbone is presented in Fig. 1a. We think that the replacement of thiophene spacer unit located in between the DPPD units of TBDPPD with thieno[3,2-b]thiophene might enhance the photovoltaic performances of resulting wide band gap polymers via the improved S–O interactions as shown in Fig. 1b. In this instance, we prepared a new polymer, P(BDTT-TTBDPPD), incorporating BDTT and novel thieno[3,2-b]thiophene incorporated BDPPD (TTBDPPD) derivatives. The opto-electrical, charge transport and photovoltaic properties of P(BDTT-TTBDPPD) are studied and briefly compared with those of P(BDTT-TBDPPD) to understand the effects of the replacement of thiophene with thieno[3,2-b]thiophene.

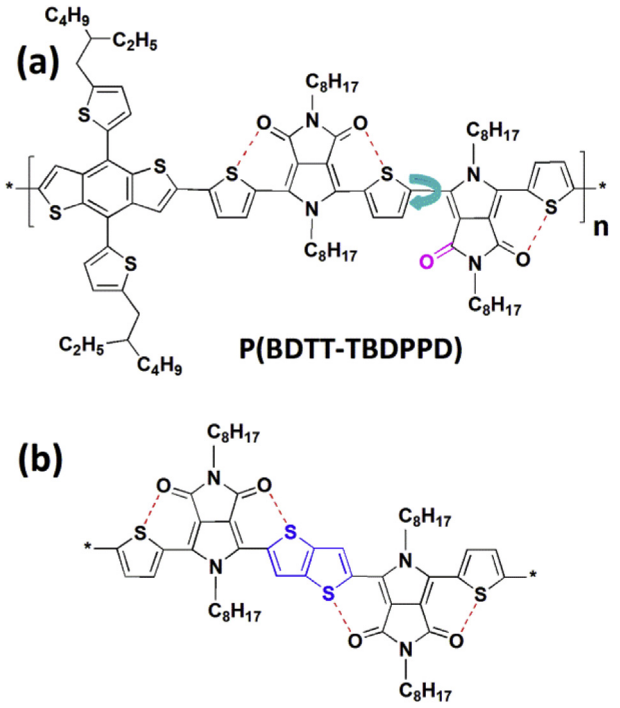

Fig. 1. Chemical structure of P(BDTT-TBDPPD) (a). The possible S–O interactions between the thienyl sulfur (S) and the carbonyl oxygen (O) on bis(pyrrolo[3,4-c]pyrrole-1,3-dione) derivatives incorporating thiophene (a) and thieno[3,2-b]thiophene (b) as a connecting spacer units.

2. Experimental section

2.1. Materials and measurements

Reagents were obtained from Sigma-Aldrich. The compounds prepared in this study were purified by column chromatography (silica gel, Merck Kieselgel 60, 70–230 mesh ASTM). The nuclear magnetic resonance (NMR) spectra of the compounds and polymer were recorded on a Varian Mercury Plus spectrometer (300 MHz for ^{1}H and 75 MHz for ^{13}C). The high resolution fast atom bombardment (FAB) mass spectra of the compounds were analyzed using a JEOL JMS-700 mass spectrometer. An Agilent 1200 Infinity Series separation module was used to determine the molecular weights of the polymer using gel permeation chromatography (GPC) with chloroform as an eluent at ambient temperature. The GPC instrument was calibrated with the polystyrene standard prior to analysis. The film state UV–visible absorption spectrum of the polymer was recorded on a JASCO V-570 spectrophotometer, and a CH Instruments Electrochemical Analyzer was used to determine the cyclic voltammogram (CV) of the polymer. The polymer cast film on the platinum working electrode was immersed in an acetonitrile solution containing 0.1 M tetrabutylammonium tetrafluoroborate (Bu_4NBF_4), Ag/AgCl as a reference electrode and platinum wire as a counter electrode, and the measurement was then performed. Before starting the CV analysis, the instrument was calibrated with the most common ferrocene/ferrocenium ion (Fc/Fc^{+}) standard. Atomic force microscopy (AFM) was performed using a Seiko instruments SPI 3800N-SPA 400.

2.2. Device fabrication and characterization of OFETs

The organic field effect transistors (OFETs) were fabricated on highly n-type-doped silicon (Si) substrates with a 200 nm layer of thermally grown silicon oxide (SiO_2). The Si substrates were subjected to an UV-ozone treatment for 30 min for activation and then treated with an octadecyltrichlorosilane (OTS) self-assembled monolayer. The n-type doped Si substrate functions as a gate electrode and the SiO_2 layer acts as a gate dielectric. The chlorobenzene (CB) solution of the polymer (5 mg/mL) was spin-cast on top of the Si substrate (2000 rpm) and dried at room temperature (RT) for 30 min. The source and drain electrodes (Au, 70 nm) were deposited on top of the polymer layer by thermal evaporation in a vacuum of approximately 2×10^{-6} Torr. The channel length (L) and channel width (W) of the device was 50 μm and 3.0 mm, respectively. The output and transfer characteristics of the OFETs were measured using a Keithley semiconductor parametric analyzer (Keithley 4200). All preparation processes and the characterization of the OFETs were performed inside a N_2-atmosphere glove box. The mobility (μ) was determined using the following equation in the saturation regime:

$$I_{DS,sat} = \mu(WC_i/2L)(V_{GS} - V_T)^2$$

where C_i is the capacitance per unit area of the SiO_2 dielectric ($C_i = 15$ nF cm^{-2}) and V_T is the threshold voltage.

2.3. Device fabrication and characterization of PSCs

The PSCs were fabricated with the simple device structure of ITO-coated glass substrate/PEDOT:PSS/P(BDTT-TTBDPPD):$PC_{70}BM$/Al. The pre-cleaned ITO-coated glass substrate was dried overnight in an oven. A 40 nm thick layer of PEDOT:PSS (Baytron PH) was spin-cast from an aqueous solution on an ITO-coated glass substrate. The substrate was dried for 10 min at 140 °C in air and then transferred to a glove box to spin-cast the photoactive layer. A

solution containing a mixture of P(BDTT-TTBDPPD):$PC_{70}BM$ (1:1, 1:2, 1:3 and 1:4 wt%) with a total concentration of 20 mg/mL in chlorobenzene (CB): 1,8-diiodoctane (DIO) at a volume ratio of 97:3 (CB: DIO) was then spin-cast on top of the PEDOT/PSS layer. The film was then dried for 30 min at RT in the glove box. Subsequently, an aluminum (Al, 100 nm) electrode was deposited by thermal evaporation in a vacuum of approximately 3×10^{-6} Torr. The current density-voltage (J–V) characteristics of the PSC devices were measured using a Keithley 2400 Source Measure Unit. The solar cell performance was determined using an Air Mass 1.5 Global (AM 1.5 G) solar simulator with an irradiation intensity of 1000 Wm^{-2}. The spectral mismatch factor was calculated by comparing the solar simulator spectrum with the AM 1.5 spectrum at RT.

2.4. Synthesis of polymers

2.4.1. Synthesis of tetraethyl 2,2'-(thieno[3,2-b]thiophene-2,5-diyl) bis(1-octyl-1H-pyrrole-3,4-dicarboxylate) (**2**)

A solution of diethyl 2-bromo-1-octyl-1H-pyrrole-3,4-dicarboxylate (**1**, 1.89 g, 4.72 mmol), which was prepared using the reported procedure,[36] and bis(trimethylstannyl)-thieno[3,2-b] thiophene (1.00 g, 2.15 mmol) in toluene (50 mL) was purged with argon for 45 min, and $Pd(PPh_3)_4$ (2 mol %) was then added. The stirred solution was heated to reflux for 15 h under an argon atmosphere. The solution was cooled and the solvent was then removed completely using a rotary evaporator. The residue was dissolved in ethyl acetate (100 mL), washed with a brine solution, and dried over anhydrous Na_2SO_4. The solvent was removed and the compound was purified by column chromatography (silica gel, hexane:ethyl acetate, 60/40, v/v) to afford pure product **2**. Yield: 1.27 g (76%). ^{1}H NMR (300 MHz, $CDCl_3$, δ): 7.65 (s, 2H), 7.35 (s, 2H), 4.24 (q, 8H), 3.89 (t, 4H), 1.69 (t, 4H), 1.35–1.16 (m, 32H), 0.85 (t, 6H); ^{13}C NMR (75 MHz, $CDCl_3$, δ): 165.1, 163.5, 140.0, 132.1, 127.7, 127.2, 122.4, 118.5, 115.0, 60.9, 60.3, 47.9, 31.7, 31.2, 29.0, 26.5, 22.6, 14.4, 14.1, 14.0; HRMS (ESI) m/z: $[M + H]^+$ calcd for $C_{42}H_{58}N_2O_8S_2$, 782.3635; found, 782.3641.

2.4.2. Synthesis of tetraethyl 5,5'-(thieno[3,2-b]thiophene-2,5-diyl) bis(2-bromo-1-octyl-1H-pyrrole-3,4-dicarboxylate) (**3**)

NBS (0.64 g, 3.57 mmol) was added in one portion to a stirred solution of compound **2** (1.27 g, 1.62 mmol) in 30 mL of DMF at RT. The solution was stirred for 3 h and then poured into water (150 mL). The solution was extracted twice with diethyl ether (50 mL) and the combined organic layer was washed once with brine and dried over anhydrous Na_2SO_4. The solvent was removed and the compound was purified by column chromatography (silica gel, hexane:ethyl acetate, 70/30, v/v) to afford pure product **3**. Yield: 1.57 g (100%). ^{1}H NMR (300 MHz, $CDCl_3$, δ): 7.30 (s, 2H), 4.40–4.10 (m, 8H), 3.96 (t, 4H), 1.69 (t, 4H), 1.39–1.13 (m, 32H), 0.86 (t, 6H); ^{13}C NMR (75 MHz, $CDCl_3$, δ): 163.9, 163.2, 140.1, 132.1, 128.2, 123.0, 118.8, 115.8, 108.9, 60.9, 47.0, 31.7, 30.8, 29.0, 28.9, 26.5, 22.6, 14.2, 14.1, 13.9; HRMS (ESI) m/z: $[M + H]^+$ calcd for $C_{42}H_{56}Br_2N_2O_8S_2$. 938.1845; found, 938.1851.

2.4.3. Synthesis of tetraethyl 5,5'-(thieno[3,2-b]thiophene-2,5-diyl) bis(1-octyl-2-(thiophen-2-yl)-1H-pyrrole-3,4-dicarboxylate) (**4**)

A solution of compound **3** (1.57 g, 1.67 mmol) and 2-(trimethylstannyl)thiophene (1.00 g, 4.00 mmol) in toluene (50 mL) was purged with argon for 45 min, and $Pd(PPh_3)_4$ (2 mol %) was then added. The stirred solution was heated under reflux for 24 h under an argon atmosphere, and the solvent was then removed completely using a rotary evaporator. The residue was dissolved in ethyl acetate (100 mL), washed with a brine solution, and dried over anhydrous Na_2SO_4. The solvent was removed and the compound was purified by column chromatography (silica gel, hexane:ethyl acetate, 60/40, v/v) to afford pure product **4**. Yield: 1.33 g (84%). ^{1}H NMR (300 MHz, $CDCl_3$, δ): 7.49 (d, 2H), 7.34–7.12 (m, 6H), 4.18 (q, 8H), 3.87 (t, 4H), 1.48 (t, 4H), 1.23–1.03 (m, 32H), 0.83 (t, 6H); ^{13}C NMR (75 MHz, $CDCl_3$, δ): 164.5, 164.3, 140.1, 132.4, 130.4, 130.1, 129.0, 128.5, 128.1, 127.0, 122.7, 117.4, 117.3, 60.6, 45.6, 31.6, 31.2, 28.8, 28.7, 26.3, 22.6, 14.1, 14.0, 13.9; HRMS (ESI) m/z: $[M + H]^+$ calcd for $C_{50}H_{62}N_2O_8S_4$, 946.3389; found, 946.3395.

2.4.4. Synthesis of tetraethyl 5,5'-(thieno[3,2-b]thiophene-2,5-diyl) bis(2-(5-bromothiophen-2-yl)-1-octyl-1H-pyrrole-3,4-dicarboxylate) (**5**)

NBS (0.55 g, 3.10 mmol) was added in one portion to a stirred solution of compound **5** (1.33 g, 1.40 mmol) in 25 mL of DMF at RT. The solution was extracted twice with diethyl ether (50 mL) and the combined organic layer was washed once with brine and dried over anhydrous Na_2SO_4. The solvent was removed and the compound was purified by column chromatography (silica gel, hexane:ethyl acetate, 60/40, v/v) to afford pure product **5**. Yield: 1.53 g (99%). ^{1}H NMR (300 MHz, $CDCl_3$, δ): 7.33 (s, 2H), 7.00–6.95 (m, 4H), 4.18 (q, 8H), 3.88 (t, 4H), 1.49 (t, 4H), 1.22–1.07 (m, 32H), 0.84 (t, 6H); ^{13}C NMR (75 MHz, $CDCl_3$, δ): 164.2, 164.0, 140.1, 132.2, 131.7, 131.0, 130.0, 128.6, 127.9, 127.1, 122.7, 117.7, 114.7, 60.8, 45.6, 31.6, 31.2, 28.8, 28.7, 26.3, 22.6, 14.1, 14.0, 13.9; HRMS(ESI) m/z: $[M + H]^+$ calcd for $C_{50}H_{60}Br_2N_2O_8S_4$, 1102.1599; found, 1102.1605.

2.4.5. Synthesis of 5,5'-(thieno[3,2-b]thiophene-2,5-diyl)bis(2-(5-bromothiophen-2-yl)-1-octyl-1H-pyrrole-3,4-dicarboxylic acid) (**6**)

An aqueous sodium hydroxide (1.10 g in 10 mL water, 28.00 mmol) solution was added to the stirred solution of compound **5** (1.53 g, 1.38 mmol) in methanol: tetrahydrofuran (60:30 mL). The solution was heated to 60 °C and stirred for 12 h. Methanol was then removed by rotary evaporation and the remaining residue was dissolved in water (100 mL). The aqueous solution was acidified with 2 N HCl until it became acidic. Then, the mixture was extracted twice with ethyl acetate (50 mL) and the combined organic layer was washed once with water and dried over anhydrous Na_2SO_4. The solvent was removed and the solid material was washed with hexane to afford pure product **6**. Yield: 1.05 g (76%). ^{1}H NMR (300 MHz, $CDCl_3$, δ): 7.31 (s, 2H), 7.26 (d, 2H), 7.12 (d, 2H), 4.13 (q, 4H), 1.90–2.10 (s, 4H), 1.28–1.06 (m, 20H), 0.84 (t, 6H); HRMS (ESI) m/z: $[M + H]^+$ calcd for $C_{42}H_{44}Br_2N_2O_8S_4$, 990.0347; found, 990.0353.

2.4.6. Synthesis of 6,6'-(thieno[3,2-b]thiophene-2,5-diyl)bis(4-(5-bromothiophen-2-yl)-5-octyl-1H-furo[3,4-c]pyrrole-1,3(5H)-dione) (**7**)

A solution of compound **6** (1.05 g, 1.06 mmol) in acetic anhydride (60 mL) was stirred at 80 °C overnight. Acetic anhydride was removed completely and the residue was dissolved in ethyl acetate (100 mL). The organic solution was washed once with an aqueous sodium bicarbonate solution (5%) and the organic layer was then dried over anhydrous Na_2SO_4. The solvent was removed and the solid material was washed with hexane to afford pure product **7**. Yield: 0.66 g (66%). ^{1}H NMR (300 MHz, $CDCl_3$, δ): 7.30–7.20 (m, 4H), 7.00 (d, 2H), 4.13 (q, 4H), 1.90–2.10 (m, 4H), 1.28–1.06 (m, 20H), 0.84 (t, 6H); HRMS (ESI) m/z: $[M + H]+$ calcd for $C_{42}H_{40}Br_2N_2O_6S_4$, 954.0136; found, 954.0142.

2.4.7. Synthesis of 6,6'-(thieno[3,2-b]thiophene-2,5-diyl)bis(4-(5-bromothiophen-2-yl)-2,5-dioctylpyrrolo[3,4-c]pyrrole-1,3(2H,5H)-dione) (TTBDPPD)

To the ice cold solution of compound **7** (0.44 g, 0.46 mmol) in anhydrous toluene (50 mL) was added 2-octyldodecan-1-amine (0.33 g, 1.10 mmol, in 5 mL toluene) drop-wise through a syringe under an argon atmosphere. The solution was stirred for 1 h at 0 °C

and then heated slowly under reflux overnight. Toluene was removed completely and the residue was dissolved in dry methylene chloride (50 mL) and cooled to 0 °C. To the stirred solution, 5 mL of thionyl chloride was added in one portion and heated to 40 °C. After 30 min, the solution was removed completely by rotary evaporation. The pasty mass was dissolved in methylene chloride (50 mL) and washed with brine. The organic layer was dried over anhydrous Na_2SO_4. The solvent was concentrated and the residue was then purified by column chromatography (silica gel, methylene chloride) to afford pure product BTBDPPD. Yield: 0.47 g (67%). ^{1}H NMR (300 MHz, $CDCl_3$, δ): 8.10 (s, 2H), 7.54 (d, 2H), 7.16 (d, 2H), 4.36 (t, 4H), 3.47 (d, 4H), 1.88–1.74 (m, 6H), 1.25 (s, 84H), 0.88 (t, 18H); ^{13}C NMR (75 MHz, $CDCl_3$, δ): 164.4, 164.0, 140.5, 131.9, 131.0, 130.8, 130.4, 127.2, 126.3, 122.9, 119.1, 119.0, 115.1, 47.0, 42.5, 37.2, 31.9, 31.7, 31.6, 31.3, 30.0, 29.7, 29.6, 29.4, 29.3, 29.1, 28.9, 26.5, 26.3, 22.7, 22.6, 14.2; HRMS (ESI) m/z: $[M + H]^+$ calcd for $C_{82}H_{122}Br_2N_4O_4S_4$, 1512.6716; found, 1512.6722.

2.4.8. Synthesis of polymer P(BDTT-TTBDPPD)

A flame dried three neck round bottom flask containing a solution of monomers BDTT (0.18 g, 0.20 mmol) and TTBDPPD (0.30 g, 0.20 mmol) in CB (20 mL) was purged well with argon for 30 min. Subsequently, Pd_2dba_3 (28 mg) and P(o-tol)$_3$ (56 mg) were added and the entire mixture was heated under reflux in argon for 36 h. The solution was cooled to RT and the solution was added drop wise to methanol (250 mL) with constant stirring. The precipitated polymer was then allowed to settle. The precipitates were filtered and washed sequentially with methanol (50 mL) and acetone (50 mL). The polymer was then subjected to Soxhlet extraction with methanol and acetone for 24 h. The remaining solid was dried under vacuum to afford pure polymer P(BDT-BTBDPPD) as a brown solid. Yield (0.38 g, 98%). ^{1}H NMR (300 MHz, $CDCl_3$, δ): 7.82–7.63 (m, 4H), 7.26–7.48 (m, 4H), 6.80–7.0 (m, 4H), 4.50 (s, 4H), 3.48 (s, 4H), 2.89 (s, 4H), 1.97–1.10 (m, 108H), 1.00–0.85 (m, 30H).

3. Results and discussions

3.1. Synthesis and characterization of polymer

The synthetic routes to new electron deficient monomer, 6,6'-(thieno[3,2-b]thiophene-2,5-diyl)bis(4-(5-bromothiophen-2-yl)-2,5-dioctylpyrrolo[3,4-c]pyrrole-1,3(2H,5H)-dione) (TTBDPPD), and polymer P(BDTT-TTBDPPD) are outlined in Scheme 1. The solubility of P(BDTT-TTBDPPD) was found to be good in chloroform, CB, and dichlorobenzene (DCB). The estimated weight average (M_w), number average (M_n) molecular weights and polydispersity

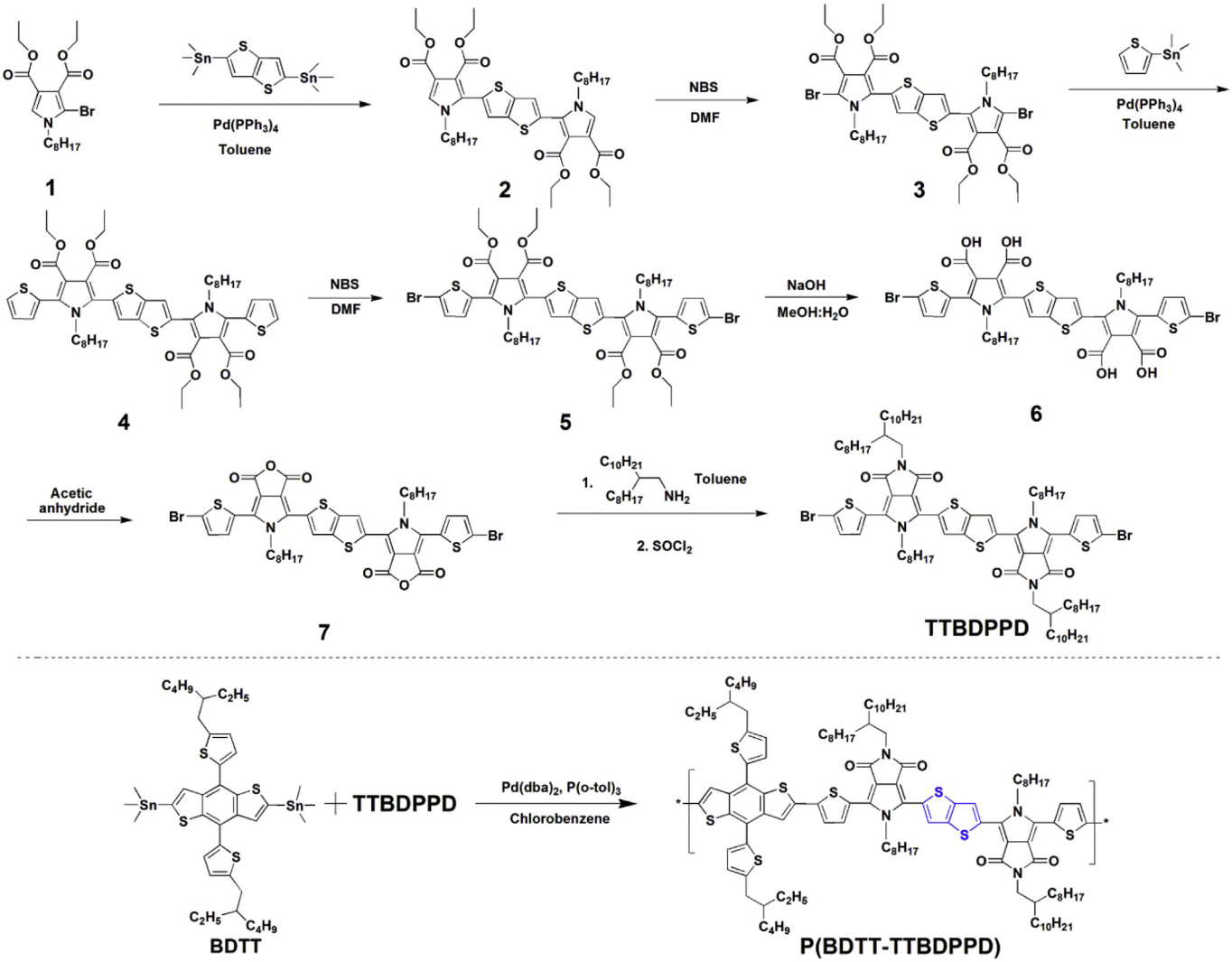

Scheme 1. Synthetic route to monomer TTBDPPD and polymer P(BDTT-TTBDPPD).

Table 1
Molecular weights, opto-electrical and charge transport properties of polymers P(BDT-TBDPPD) and P(BDTT- TTBDPPD).

Polymer name	M_w (g/mol)[b]	PDI[b]	λ_{max} as film (nm)[c]	E_g (eV)[d]	HOMO (eV)[e]	LUMO (eV)[f]	μ ($cm^2V^{-1}s^{-1}$)[g]
P(BDTT-TBDPPD)[a]	2.57×10^4	1.88	505	2.08	−5.44	−3.36	3.20×10^{-4}
P(BDTT-TTBDPPD)	1.69×10^5	3.67	505	2.06	−5.42	−3.36	6.21×10^{-4}

[a] Data for P(BDTT-TBDPPD) are quoted from Ref. [36].
[b] Weight average molecular weight (M_w) and polydispersity (PDI) of the polymers were determined by GPC using polystyrene standards.
[c] Measurements in thin film were performed on the glass substrate.
[d] Band gap estimated from the onset wavelength of the optical absorption in thin film.
[e] The HOMO level was estimated from cyclic voltammetry analysis.
[f] The LUMO level was estimated by using the following equation: LUMO = HOMO + E_g.
[g] The hole mobility of polymers were estimated from organic filed effect transistors.

(PDI) of P(BDTT-TTBDPPD) were 1.69×10^5 g/mol, 4.60×10^4 g/mol and 3.67, respectively. The M_w and PDI of P(BDTT-TTBDPPD) are listed in Table 1 along with those of P(BDTT-TBDPPD) for comparison.

3.2. Optical properties

The absorption spectra of polymers P(BDTT-TBDPPD) and P(BDTT-TTBDPPD) were recorded as thin films on glass under identical conditions and presented in Fig. 2a. It is very clear P(BDTT-TTBDPPD) showed higher absorption coefficient and relatively broad and red shift absorption band compared to that of P(BDTT-TBDPPD). However, both polymers exhibited identical absorption maximum (~505 nm) values. The calculated optical band gap (E_g) of P(BDTT-TTBDPPD) was 2.06 eV, and which is slightly lower than that of P(BDTT-TBDPPD). The broad band width of P(BDTT-TTBDPPD) suggests that the planarity of P(BDTT-TTBDPPD) is higher than that of P(BDTT-TBDPPD). Therefore we think that the vibronic peak at around 545 nm is originated from the localized π−electrons rather than molecular interchain interactions of polymers.

The π−electrons are delocalized well on P(BDTT-TTBDPPD) backbone due to their increased planarity, and consequently the peak attributed from localized π−electrons (vibronic peak at around 545 nm) disappeared compared to that of P(BDTT-TBDPPD). The DFT calculation performed for monomers TBDPPD and TTBDPPD using B3LYP hybrid functional and 6-31G* basis sets confirmed that TTBDPPD is more planar than TBDPPD. The optimized structures of TBDPPD and TTBDPPD are shown in Fig. 2b. It is very clear from the optimized structures that the two DPPD units are in different planes on TBDPPD, but they are in the almost identical planes on TTBDPPD. Consequently, the planarity of P(BDTT-TTBDPPD) is expected to be higher than that of P(BDTT-TBDPPD).

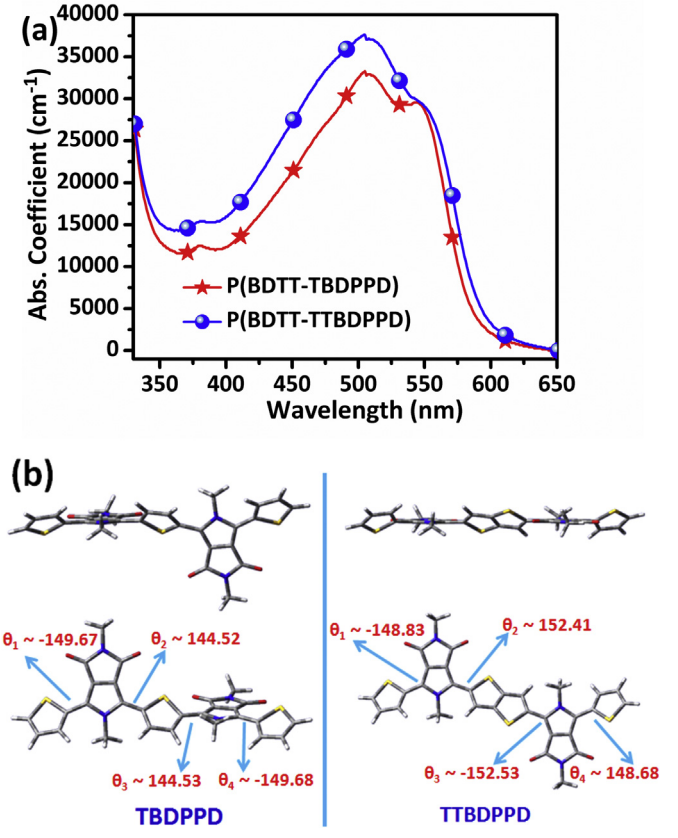

Fig. 2. (a) Film state absorption spectra of P(BDTT-TBDPPD) and P(BDTT-TTBDPPD), (b) and the optimized structures of TBDPPD and TTBDPPD.

3.3. Electrochemical properties

To determine the highest occupied and lowest unoccupied molecular orbital (HOMO and LUMO) energy levels of P(BDTT-TTBDPPD), we performed CV analysis with P(BDTT-TTBDPPD) as described in experiment section. The CV spectrum of P(BDTT-TTBDPPD) is presented in Fig. 3. The estimated onset oxidation potentials of P(BDTT-TTBDPPD) ($E_{ox,onset\ vs.\ Ag/AgCl}$) and standard ferrocene ($E_{ferrocene\ vs.\ Ag/AgCl}$) were 1.10 V and 0.48 V, respectively. The HOMO and LUMO energy levels of P(BDTT-TTBDPPD) calculated using the standard equation, $E_{HOMO} = [-(E_{ox,onset\ vs.\ Ag/AgCl} - E_{ferrocene\ vs.\ Ag/AgCl}) - 4.8]$ eV and LUMO = HOMO + E_g,

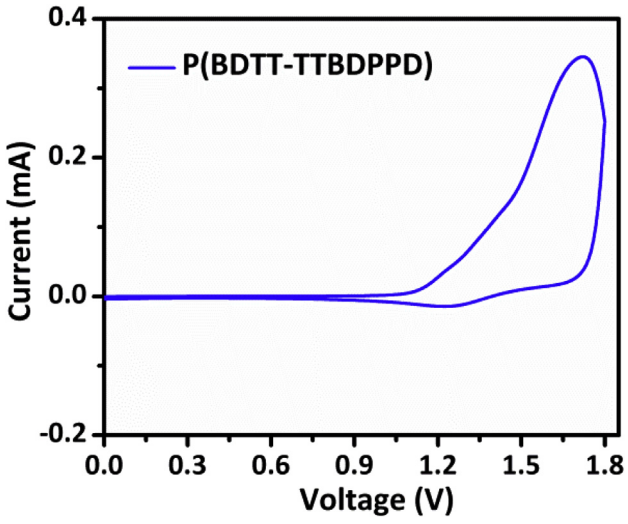

Fig. 3. Cyclic voltammogram of P(BDTT-TTBDPPD).

were −5.42 eV and −3.36 eV, respectively. The opto-electrical studies suggest that the replacement of the thiophene spacer unit located in between the DPPD units of P(BDTT-TBDPPD) with thieno [3,2-b]thiophene unit does not make notable changes on their energy levels. The absorption maximum and energy levels of P(BDTT-TBDPPD) and P(BDTT-TTBDPPD) are included in Table 1.

3.4. OFETs characteristics

The organic field effect transistor (OFETs) was prepared using P(BDTT-TTBDPPD) to estimate it's semiconducting behavior as well as hole mobility. The transfer characteristics of the OFETs are displayed in Fig. 4. The OFETs characteristics indicate that P(BDTT-TTBDPPD) is a p-type semiconductor and exhibits a maximum field-effect mobility (μ) of 6.21×10^{-4} $cm^2V^{-1}s^{-1}$. The hole mobility of P(BDTT-TTBDPPD) was higher than that of P(BDTT-TBDPPD). As stated earlier, the enhanced planarity of TTBDPPD unit via the improved S–O interactions compared to that of TBDPPD unit was expected to allow better molecular packing between the polymer chains, and consequently offered higher hole mobility. The hole

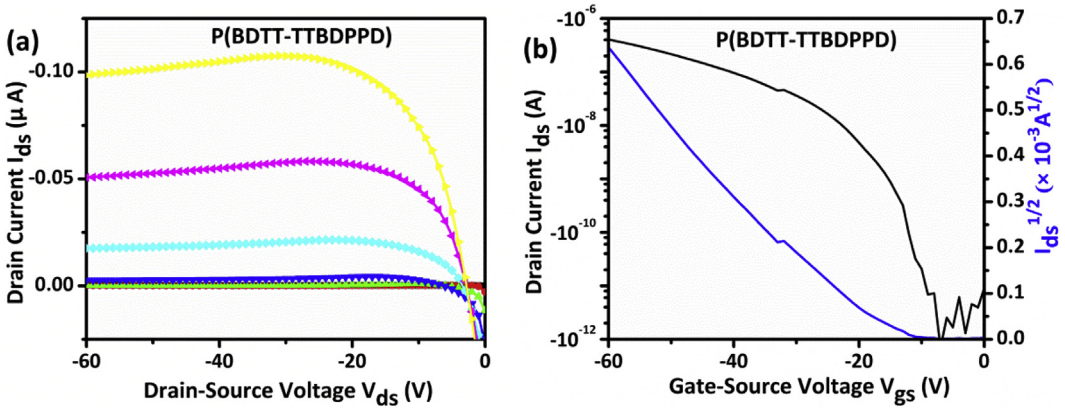

Fig. 4. Typical current–voltage characteristics (drain–source current, I_{ds}, and drain–source current, $I_{ds}^{1/2}$, versus gate–source voltage, V_{gs}, plots) for P(BDTT-TTBDPPD)-based OFETs.

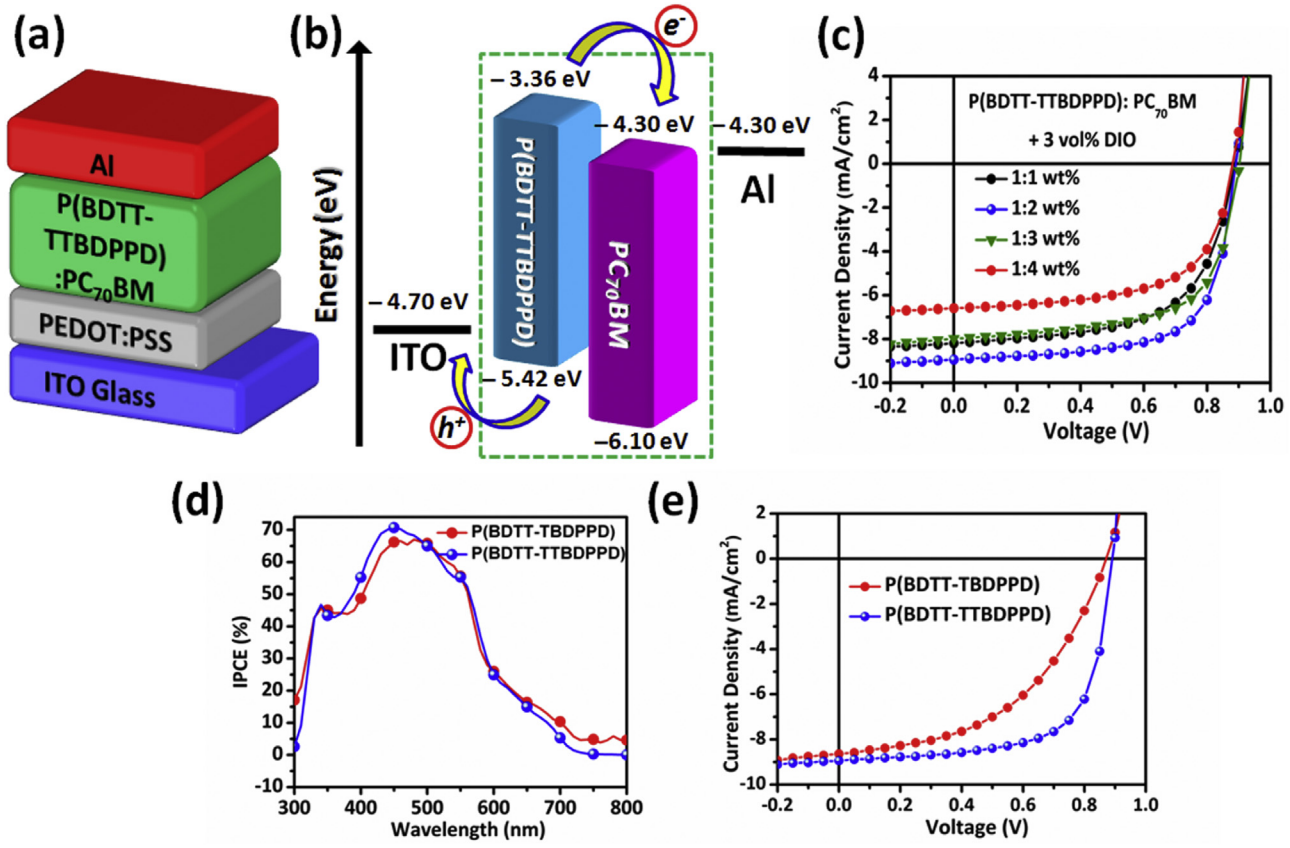

Fig. 5. The PSC device structure (a), the energy level diagram for the materials used for PSC fabrication (b), the *J–V* characteristics of the PSCs prepared using P(BDTT-TTBDPPD):$PC_{70}BM$ (at different ratio)+3 vol% DIO blends (c), the *IPCE* spectra of the PSCs made using P(BDTT-TBDPPD):$PC_{70}BM$ (1:1 wt%)+3 vol% DIO and P(BDTT-TTBDPPD):$PC_{70}BM$ (1:2 wt%)+3 vol% DIO blends (d), and the *J–V* characteristics of the PSCs made from P(BDTT-TBDPPD):$PC_{70}BM$ (1:1 wt%)+3 vol% DIO and P(BDTT-TTBDPPD):$PC_{70}BM$ (1:2 wt%)+3 vol % DIO blends (e).

mobilities of P(BDTT-TBDPPD) and P(BDTT-TTBDPPD) are included in Table 1.

3.5. BHJ solar cell properties

The photovoltaic performance of P(BDTT-TTBDPPD) was examined by making PSCs with P(BDTT-TTBDPPD) as an electron donor and $PC_{70}BM$ as an electron acceptor. The PSC device structure and its energy level diagram are shown in Fig. 5a and b, respectively. The *J-V* curves of the PSCs made from P(BDTT-TTBDPPD):$PC_{70}BM$ + 3 vol% DIO blends at four different ratios, 1:1 wt%, 1:2 wt% and 1:3 wt%, are displayed in Fig. 5c, and their corresponding photovoltaic parameters such as *PCE*, V_{oc}, J_{sc} and *FF* are summarized in Table 2. Among them, the PSCs made from P(BDTT-TTBDPPD):$PC_{70}BM$ (1:2 wt%)+ 3 vol% DIO blends gave a maximum *PCE* of 5.37% with a V_{oc} of 0.90 V, a J_{sc} of 8.94 mA/cm^2, and a *FF* of 67%. Interestingly, P(BDTT-TTBDPPD) exhibit high V_{oc} and *FF*. However, the wide band gap of P(BDTT-TTBDPPD) limits the photocurrent of PSCs and restrict the *PCE* below 5.5%. The theoretical and experimental V_{oc} values are consistent with each other, and the *FF* is also found to be high compared to that of efficient polymers reported for PSCs [7–35]. In order to make sure the J_{sc} value achieved for P(BDTT-TTBDPPD), we measured the incident photon to the collected electron (*IPCE*) spectra of the PSC made using P(BDTT-TTBDPPD):$PC_{70}BM$ (1:2 wt%)+ 3 vol% DIO blend. The corresponding *IPCE* spectrum is shown in Fig. 5d. The *IPCE* curves cover the region from 300 nm to 700 nm with maximum *IPCE* of 71%. The integrated J_{sc} value (~8.71 mA/cm^2) of *IPCE* curve is quite similar to that of the J_{sc} obtained from *J-V* curve. We also measured the atomic force microscopy (AFM) images of the films made from P(BDTT-TTBDPPD):$PC_{70}BM$ (1:2 wt%)+ 3 vol% DIO blends to study the surface morphology of the photoactive layer because the morphology play a vital role on the photovoltaic performances of PSCs. The topology, phase and 3D topology AFM images of the films are presented in Fig. 6. The AFM images reveal that the blending between P(BDTT-TTBDPPD) and $PC_{70}BM$ is excellent with less root mean square (rms, ~0.42 nm) roughness. In addition, the high grains observed in 3D topology image are favourable for efficient charge transports via the improved contacts between photoactive layer and cathode.

The reported *PCE* for the PSC device made under the similar condition with structurally quite similar wide band gap polymer P(BDTT-TBDPPD) (see Fig. 1) was 3.63% (V_{oc} ~ 0.87 V, J_{sc} ~ 8.64 mA/cm^2, and *FF* ~ 48%) [36]. The comparison of the photovoltaic performance of P(BDTT-TBDPPD) and P(BDTT-TTBDPPD) evidenced that the *PCE* of P(BDTT-TBDPPD) has been greatly improved (~2%) just replacing the thiophene spacer unit positioned between the DPPD units with thieno[3,2-b]thiophene. The *J-V* curves of the PSCs made using P(BDTT-TBDPPD):$PC_{70}BM$ (1:1 wt%)+3 vol% DIO and P(BDTT-TTBDPPD):$PC_{70}BM$ (1:2 wt%)+3 vol% DIO blends are shown in Fig. 5e for comparison. The HOMO levels of both polymers P(BDTT-TTBDPPD) and P(BDTT-TBDPPD) are quite similar, and consequently there was no big difference in the V_{oc} between the PSCs made from P(BDTT-TTBDPPD) and P(BDTT-TBDPPD). However, the notably improved *FF* along with the little increment in the J_{sc} remarkably enhances the overall *PCE* of P(BDTT-TTBDPPD)-based PSC compared to that of P(BDTT-TBDPPD)-based PSC. The IPCE responses are found to be higher for P(BDTT-TTBDPPD)-based PSC compared to that of P(BDTT-TBDPPD)-based PSC, and consequently the higher J_{sc} obtained for P(BDTT-TTBDPPD) is acceptable. The *IPCE* spectra of the PSCs made using P(BDTT-TBDPPD):$PC_{70}BM$ (1:1 wt %)+3 vol% DIO and P(BDTT-TTBDPPD):$PC_{70}BM$ (1:2 wt%)+3 vol%

Table 2
Photovoltaic properties of the PSCs prepared using the configuration of ITO/PEDOT:PSS/P(BDTT- TBDPPD) or P(BDTT- TTBDPPD):$PC_{70}BM$ (at different ratio)+ 3 vol% DIO/Al.

Active layer	Thickness (nm)	V_{oc} (V)[b]	J_{sc} (mA/cm^2)[c]	FF (%)[d]	PCE_{max} (%)[e]	PCE_{avg} (%)[f]
P(BDTT-TBDPPD): $PC_{70}BM$ (1:1 wt%)[a]	80	0.87	8.64	48	3.63	3.39 ± 0.24
P(BDTT- TTBDPPD):$PC_{70}BM$ (1:1 wt%)	85	0.89	8.19	61	4.44	4.26 ± 0.18
P(BDTT- TTBDPPD):$PC_{70}BM$ (1:2 wt%)	83	0.90	8.94	67	5.37	5.21 ± 0.16
P(BDTT- TTBDPPD):$PC_{70}BM$ (1:3 wt%)	82	0.90	7.99	64	4.62	4.49 ± 0.13
P(BDTT- TTBDPPD):$PC_{70}BM$ (1:4 wt%)	80	0.89	6.59	62	3.63	3.51 ± 0.12

[a] Data for P(BDTT-TBDPPD) are quoted from Ref. [36].
[b] Open-circuit voltage.
[c] Short-circuit current density.
[d] Fill factor.
[e] Power conversion efficiency.
[f] Average PCE values for five devices.

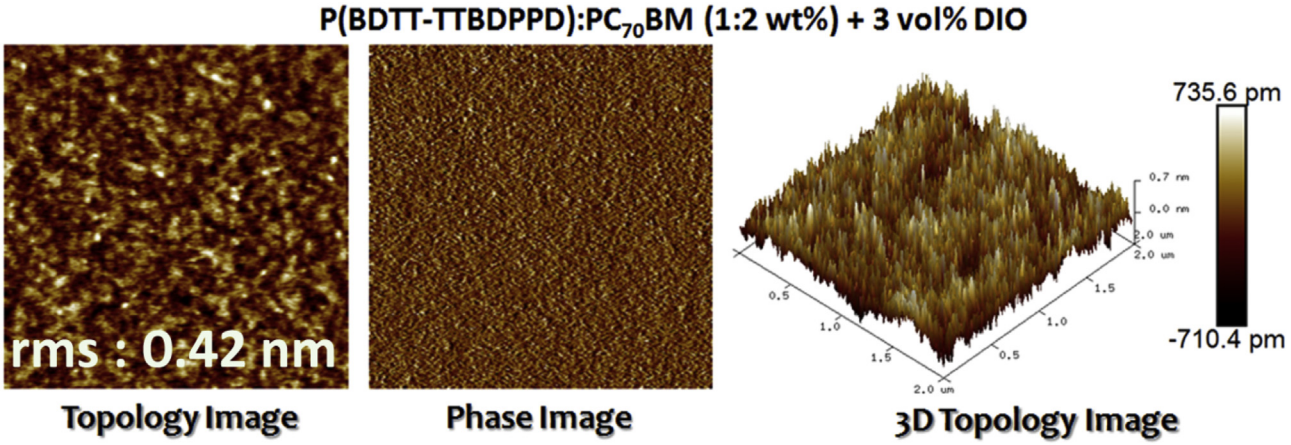

Fig. 6. Topology, phase, and 3D topology AFM images of the films made from P(BDTT-TTBDPPD):$PC_{70}BM$ (1:2 wt%)+3 vol% DIO blends.

DIO blends are shown in Fig. 5d for comparison. The *FF* is usually correlated with the molecular weights or carrier mobility of the donor polymer. In general, it is believed that the high molecular weight of polymer is favourable for efficient charge transport than that of their corresponding low molecular weight polymers. However, polymers P(BDTT-TBDPPD) and P(BDTT-TTBDPPD) showed quite similar hole mobility though their molecular weights are different. So, we think that the higher FF for P(BDTT-TTBDPPD) based device is hardly related to molecular weight or carrier mobility of the polymer. Some other reasons such as molecular packing (molecular orientation) of polymer, surface morphology of the photoactive layer and resistance of the device are more crucial factors. We think that the improved planarity could be a crucial factor for the high *FF* obtained for P(BDTT-TTBDPPD) based device. In addition, the surface morphology of the film made from P(BDTT-TTBDPPD):$PC_{70}BM$ blend is much better than the film made form P(BDTT-TBDPPD):$PC_{70}BM$. Especially, the nano scale network formation between P(BDTT-TTBDPPD) and $PC_{70}BM$ was found be excellent along with relatively smaller domain size and smooth surface compared to that of P(BDTT-TBDPPD) and $PC_{70}BM$ [36]. The companied effects support the higher *FF* achieved for P(BDTT-TTBDPPD)-based PSC compared to that of P(BDTT-TBDPPD)-based PSC. It is worth to note the photovoltaic performance of P(BDTT-TTBDPPD) is similar to that of efficient large band gap poly(3-hexylthiophene) (P3HT) [41]. In case of ternary and tandem PSCs, P3HT is widely used to harvest the high energy part of sunlight along with low band gap polymers [25,27,42]. We believe, P(BDTT-TTBDPPD) could be an efficient alternative for P3HT to make ternary and tandem PSCs along with low band gap polymers.

4. Conclusions

Bis(pyrrolo[3,4-c]pyrrole-1,3(2H,5H)-dione) (BDPPD)-based new electron deficient monomer unit (TTBDPPD) was prepared as a high energy converting wide band gap polymer for PSCs. The copolymerization of benzodithiophene (BDTT) and TTBDPPD derivative gave new polymer P(BDTT-TTBDPPD). Polymer P(BDTT-TTBDPPD) covers the absorption in the range of 300–600 nm with an optical band gap of 2.06 eV. The estimated HOMO and LUMO levels of P(BDTT-TTBDPPD) were −5.42 eV and −3.36 eV. The conventional OFETs and PSCs made using P(BDTT-TTBDPPD) exhibited a hole mobility and maximum *PCE* of $6.21 \times 10^{-4}\ cm^2V^{-1}s^{-1}$ and 5.37%, respectively. We confirm that the replacement of thiophene spacer unit placed between the DPPD units of BDPPD with thieno[3,2-b]thiophene does not alter the energy levels of resulting polymer much, but the notably improved absorption, hole mobility and surface morphology of the photoactive layer greatly enhances the overall *PCE*. This study clearly evidenced that the spacer unit positioned between the DPPD units of BDPPD is crucial to get efficient polymers for PSCs. We believe that P(BDTT-TTBDPPD) could be a promising wide band gap polymers to utilize in ternary and tandem PSCs.

Acknowledgements

This research was supported by the National Research Foundation of Korea (NRF-2013R1A2A2A04014576). S. C. acknowledges the support by the National Research Foundation of Korea (NRF-2014R1A4A1071686).

References

[1] L. Lu, T. Zheng, Q. Wu, A.M. Schneider, D. Zhao, L. Yu, Chem. Rev. 115 (2015) 12666.
[2] X. Guo, A. Facchetti, T.J. Marks, Chem. Rev. 114 (2014) 8943.
[3] C. Gao, L. Wang, X. Li, H. Wang, Polym. Chem. 5 (2014) 5200.
[4] P. Deng, Q. Zhang, Polym. Chem. 5 (2014) 3298.
[5] A. Pron, M. Leclerc, Prog. Polym. Sci. 38 (2013) 1815.
[6] L. Huo, J. Hou, Polym. Chem. 2 (2011) 2453.
[7] J. You, L. Dou, K. Yoshimura, T. Kato, K. Ohya, T. Moriarty, K. Emery, C.-C. Chen, J. Gao, G. Li, Y. Yang, Nat. Commun. 4 (2013) 1446.
[8] Z. He, B. Xiao, F. Liu, H. Wu, Y. Yang, S. Xiao, C. Wang, T.P. Russell, Y. Cao, Nat. Photonics. 9 (2015) 174.
[9] J.-D. Chen, C. Cui, Y.-Q. Li, L. Zhou, Q.-D. Ou, C. Li, Y. Li, J.-X. Tang, Adv. Mater. 27 (2015) 1035.
[10] L. Dou, J. Gao, E. Richard, J. You, C.-C. Chen, K.C. Cha, Y. He, G. Li, Y. Yang, J. Am. Chem. Soc. 134 (2012) 10071.
[11] L. Dou, W.-H. Chang, J. Gao, C.-C. Chen, J. You, Y. Yang, Adv. Mater. 25 (2013) 825.
[12] E. Wang, W. Mammo, M.R. Andersson, Adv. Mater. 26 (2014) 1801.
[13] J. Zhao, Y. Li, G. Yang, K. Jiang, H. Lin, H. Ade, W. Ma, H. Yan, Nat. Energy. 1 (2016) 15027.
[14] C. Duan, A. Furlan, J.J.V. Franeker, R.E.M. Willems, M.M. Wienk, R.A.J. Janssen, Adv. Mater. 27 (2015) 4461.
[15] Y. Liu, J. Zhao, Z. Li, C. Mu, W. Ma, H. Hu, K. Jiang, H. Lin, H. Ade, H. Yan, Nat. Commun. 5 (2014) 5293.
[16] K. Li, Z. Li, K. Feng, X. Xu, L. Wang, Q. Peng, J. Am. Chem. Soc. 135 (2013) 13549.
[17] J.-H. Kim, J.B. Park, I.H. Jung, A.C. Grimsdale, S.C. Yoon, H. Yang, D.-H. Hwang, Energy Environ. Sci. 8 (2015) 2352.
[18] N. Wang, Z. Chen, W. Wei, Z. Jiang, J. Am. Chem. Soc. 135 (2013) 17060.
[19] C.-C. Chen, W.-H. Chang, K. Yoshimura, K. Ohya, J. You, J. Gao, Z. Hong, Y. Yang, Adv. Mater. 26 (2014) 5670.
[20] J.-H. Kim, J.B. Park, F. Xu, D. Kim, J. Kwak, A.C. Grimsdale, D.-H. Hwang, Energy Environ. Sci. 7 (2014) 4118.
[21] J. Youa, L. Doua, Z. Hongc, G. Li, Y. Yang, Prog. Polym. Sci. 38 (2013) 1909.
[22] W. Li, A. Furlan, K.H. Hendriks, M.M. Wienk, R.A.J. Janssen, J. Am. Chem. Soc. 135 (2013) 5529.
[23] L. Dou, J. You, J. Yang, C.-C. Chen, Y. He, S. Murase, T. Moriarty, K. Emery, G. Li, Y. Yang, Nat. Photonic. 6 (2012) 180.
[24] J. You, L. Dou, K. Yoshimura, T. Kato, K. Ohya, T. Moriarty, K. Emery, C.-C. Chen, J. Gao, G. Li, Y. Yang, Nat. Commun. 4 (2013) 1446.
[25] L. Lu, M.A. Kelly, W. You, L. Yu, Nat. Photonics. 9 (2015) 491.
[26] L. Lu, T. Xu, W. Chen, E.S. Landry, L. Yu, Nat. Photonics. 8 (2014) 716.
[27] T. Ameri, P. Khoram, J. Min, C.J. Brabec, Adv. Mater. 25 (2013) 4245.
[28] P. Cheng, Y. Li, X. Zhan, Energy Environ. Sci. 7 (2014) 2005.
[29] L. Lu, T. Xu, W. Chen, E.S. Landry, L. Yu, Nat. Photonics. 8 (2014) 716.
[30] T. Ameri, P. Khoram, J. Min, C.J. Brabec, Adv. Mater. 25 (2013) 4245.
[31] X. Guo, C. Cui, M. Zhang, L. Huo, Y. Huang, J. Hou, Y. Li, Energy Environ. Sci. 5 (2012) 7943.
[32] S.H. Park, A. Roy, S. Beaupŕe, S. Cho, N. Coates, J.S. Moon, D. Moses, M. Leclerc, K. Lee, A.J. Heeger, Nat. Photonics. 3 (2009) 297.
[33] W. Li, L. Yang, J.R. Tumbleston, L. Yan, H. Ade, W. You, Adv. Mater. 26 (2014) 4456.
[34] V. Tamilavan, K.H. Roh, R. Agneeswari, D.Y. Lee, S. Cho, Y. Jin, S.H. Park, M.H. Hyun, J. Polym. Sci. A Polym. Chem. 52 (2014) 3564.
[35] V. Tamilavan, K.H. Roh, R. Agneeswari, D.Y. Lee, S. Cho, Y. Jin, S.H. Park, M.H. Hyun, J. Mater. Chem. A 2 (2014) 20126.
[36] R. Agneeswari, I. Shin, V. Tamilavan, D.Y. Lee, S. Cho, Y. Jin, S.H. Park, M.H. Hyun, Org. Electron. 30 (2016) 253.
[37] X. Guo, N. Zhou, S.J. Lou, J.W. Hennek, R.P. Ortiz, M.R. Butler, P.-L.T. Boudreault, J. Strzalka, P.-O. Morin, M. Leclerc, J.T.L. Navarrete, M.A. Ratner, L.X. Chen, R.P.H. Chang, A. Facchetti, T.J. Marks, J. Am. Chem. Soc. 134 (2012) 18427.
[38] N. Zhou, X. Guo, R.P. Ortiz, S. Li, S. Zhang, R.P.H. Chang, A. Facchetti, T.J. Marks, Adv. Mater. 24 (2012) 2242.
[39] C. Cabanetos, A.E. Labban, J.A. Bartelt, J.D. Douglas, W.R. Mateker, J.M.J. Frechet, M.D. McGehee, P.M. Beaujuge, J. Am. Chem. Soc. 135 (2013) 4656.
[40] C.E. Small, S. Chen, J. Subbiah, C.M. Amb, S.-W. Tsang, T.-H. Lai, J.R. Reynolds, F. So, Nat. Photonics. 6 (2012) 115.
[41] A. Marrocchi, D. Lanari, A. Facchetti, L. Vaccaro, Energy Environ. Sci. 5 (2012) 8457.
[42] J. Youa, L. Doua, Z. Hongc, G. Li, Y. Yang, Prog. Polym. Sci. 38 (2013) 1909.